A Kinetic Study of Sulfur Dioxide in Aqueous Solution with Radioactive Tracers

J. C. WANG and D. M. HIMMELBLAU

The University of Texas, Austin, Texas

A kinetic study was made of the homogeneous reactions in the sulfur dioxide-sodium bisulfite-water system, with a radioactive tracer technique. By operating this system at chemical equilibrium but at isotopic disequilibrium the influence of the diffusion of sulfur dioxide into and out of the aqueous solution could be divorced from the kinetic effects of the chemical reaction. It was then possible to follow the rate of reaction of this system by analyzing the radioactive sulfur-35 in the form of gaseous sulfur dioxide, with the Bernstein-Ballentine technique.

Data were collected at temperatures of 0° to 20°C. and at pH ranges from 1.25 to 4.3. Analysis and correlation of the experimental data by different kinetic models demonstrated that the classical reaction $SO_2 + H_2O \rightleftharpoons H^+ + HSO_3^-$ represented the experimental data best from a macroscopic viewpoint. Because of the low pH conditions employed it was not possible to obtain rate data for the reaction $SO_2 + OH^- \rightleftharpoons HSO_3$.

Forward and reverse rate constants are reported for the first time for this system.

Processes for the absorption of sulfur dioxide in aqueous solutions are of considerable importance in the sulfite pulping industry, in the recovery of waste pickle liquor, in the purification of industrial gas wastes, and similar applications. It is surprising therefore to find no data in the literature on the homogeneous kinetics of the reaction between sulfur dioxide and its aqueous solution, although considerable work has been carried out on the absorption and subsequent chemical reaction of sulfur dioxide in water, in calcium sulfite solutions, in various bases, and in salt solutions, from an overall mass transfer viewpoint (*1, 5, 11, 16, 21, 27, 28*). However none of these investigators or their predecessors attempted to distinguish between the actual rate of the chemical reaction of sulfur dioxide with aqueous solution from a chemical kinetic viewpoint and the overall rate of mass transfer which was actually measured. The technique used in this study divorced the influence of molecular and eddy diffusion of sulfur dioxide into and out of the solution, and the diffusion of the constituents in the solution, from the kinetic effects of the chemical reaction so that true reaction-rate constants could be computed from the experimental data.

The essence of the procedure, which is described in more detail in reference *26*, was to operate with the system at chemical equilibrium but isotopic disequilibrium with a radioactive tracer technique developed by Himmelblau and Babb (*13*). Tracer in the form of $NaHS^{35}O_3$ was injected into a solution containing $S^{32}O_2$, water, and $NaHS^{32}O_3$ which had been allowed to reach equilibrium under controlled conditions of temperature, pH, and pressure. Samples of solution were taken at periodic intervals after injection of the tracer. A portion of the sulfur dioxide in each sample was flashed out of solution and analyzed by the Bernstein-Ballentine technique (*3*) to determine the ratio of $S^{35}O_2$ at time t to that of a similar sample at isotopic equilibrium. (Hereinafter the radioactive species will be presented simply by the symbol *; that is S^{35} is represented by S^*.) Designating this ratio by R one can set up a linear relationship between the quantity $\ln(1 - R)$ and the time of reaction from which the reaction-rate constants could be determined.

REACTION MODELS

Some prior information was available (*4, 8, 14*) concerning the reaction mechanisms. When sulfur dioxide dissolves in water, the resulting solution possesses well-known acidic properties, conducts an electric current, and behaves as if it contained an acid. However, although the ions H_3O^+, HSO_3^-, $HS_2O_5^-$, and perhaps a small amount of $SO_3^=$ are indeed present in the solution, the undissociated free acid itself has never been isolated or shown to exist. However substantial evidence for the existence of unchanged sulfur dioxide molecules in aqueous solution has been obtained from ultraviolet, infrared, and Raman absorption spectra (*8, 9, 10, 20, 22, 23, 24, 29*).

The classical reaction relationships for the system sulfur dioxide-water can be expressed as follows:

$$SO_2(\text{gas}) \leftrightarrows SO_2(\text{soln}) \quad (1)$$

$$SO_2(\text{soln}) + H_2O \rightleftharpoons H_2SO_3 \rightleftharpoons H^+ + HSO_3^- \quad (2)$$

$$SO_2(\text{soln}) + OH^- \rightleftharpoons HSO_3^- \quad (3)$$

$$HSO_3^- \rightleftharpoons H^+ + SO_3^= \quad (4)$$

$$H^+ + OH^- \rightleftharpoons H_2O \quad (5)$$

Reaction (1), a mass transfer process, was at equilibrium when samples were taken during an experimental run and remained so during the remainder of the run, so that this reaction had no net effect on any of the others. Reaction (2) was the one for which the forward and reverse reaction rate constants were to be determined. Reactions (4) and (5) are ionic reactions, the rates of which are presumed to be of some high order of magnitude (*17*), so that they instantly come to equilibrium. Thus the reactions of the system to be studied reduced to two reversible reactions (2) and (3). However it was possible that the influence of reaction (3) was insignificant at the low pH range used in this study. This point will be discussed later on.

RATE EQUATIONS

Rate equations were developed based both on activities and on concentrations. Activities could be approximated with sufficient accuracy for engineering purposes for the system studied by multiplying the concentrations by activity coefficients secured from the data of Tartar and Garretson (*25*), Kielland (*15*), and Harned and Owen (*12*). The development of one typical rate equation will be given here; that for the others may be found in reference *26*. For reaction (2) parallel rate equations for tracer and nontracer are (in terms of activities)

$$-\frac{d(a_{SO_2})}{dt} = \frac{d(a_{HSO_3^-})}{dt} = k_F(a_{SO_2})\ (a_{H_2O}) - k_R(a_{HSO_3^-})\ (a_{H^+}) \quad (6)$$

$$-\frac{d(a_{S^*O_2})}{dt} = \frac{d(a_{HS^*O_3^-})}{dt} = k_F(a_{S^*O_2})\ (a_{H_2O}) - k_R(a_{HS^*O_3^-})\ (a_{H^+}) \quad (7)$$

When a tracer is injected into the solution, reaction (6) is at equilibrium and may be used to eliminate k_R from Equation (7) giving

$$-\frac{d(a_{S^*O_2})}{dt} = k_F(a_{S^*O_2})\ (a_{H_2O}) - k_F(a_{HS^*O_3^-})\ (a_{H^+}) \left[\frac{(a_{SO_2})\ (a_{H_2O})}{(a_{HSO_3^-})\,(a_{H^+})}\right]$$
$$= k_F(a_{H_2O}) \left\{ (a_{S^*O_2}) - (a_{SO_2}) \left[\frac{(a_{HS^*O_3^-})}{(a_{HSO_3^-})}\right]\right\} \quad (8)$$

It can be appreciated that the time needed for the establishment of isotopic equilibrium is substantial since the chemical and ionic interchange, forward and reverse, must take place many times before effective isotopic equilibrium is achieved (designated by subscript e), and the concentrations of tracer used are quite small. Since the entire system is at chemical equilibrium at the time the tracer is injected, no actual chemical change takes place when the samples are taken from the reaction vessel during each experimental run.

The activity of S^*O_2 at isotopic equilibrium $(a_{S^*O_2})_e$ is presumably a constant. Thus if both sides of Equation (8) are divided by $(a_{S^*O_2})_e$, one can bring it into the differential sign and get

$$-\frac{d\left[\dfrac{(a_{S^*O_2})}{(a_{S^*O_2})_e}\right]}{dt} = k_F(a_{H_2O}) \left[\frac{(a_{S^*O_2})}{(a_{S^*O_2})_e} - \frac{(a_{SO_2})\ (a_{HS^*O_3^-})}{(a_{S^*O_2})_e(a_{HSO_3^-})}\right] \quad (9)$$

If one assumes that the tracer activity coefficients are essentially constant, the activity ratios can be replaced by concentration ratios

$$-\frac{d\left(\dfrac{[S^*O_2]}{[S^*O_2]_e}\right)}{dt} = k_F(a_{HO_2}) \left(\frac{[S^*O_2]}{[S^*O_2]_e} - \frac{[SO_2]\,[HS^*O_3^-]}{[S^*O_2]_e\,[HSO_3^-]}\right) \quad (10)$$

Noting that the S-35 content of the solution is constant and equal to the initial amount of tracer injected into the reaction vessel, a material balance for the tracer gives (in moles per liter)

$$[S^*O_2]_i + [HS^*O_3^-]_i = [S^*O_2] + [HS^*O_3^-] = [S^*O_2]_e + [HS^*O_3^-]_e \quad (11)$$

where the subscript i signifies initial concentration.

At isotopic equilibrium

$$\frac{[HSO_3^-]_e}{[HS^*O_3^-]_e} = \frac{[SO_2]_e}{[S^*O_2]_e} \quad (12)$$

Finally, by substituting Equations (11) and (12) into (10), the rate equation for reaction (2) is obtained:

$$-\frac{d\left(\dfrac{[S^*O_2]}{[S^*O_2]_e}\right)}{dt} = k_F(a_{H_2O}) \left(1 + \frac{[SO_2]}{[HSO_3^-]}\right) \left(\frac{[S^*O_2]}{[S^*O_2]_e} - 1\right) \quad (13)$$

or

$$-\frac{dR}{dt} = k_F(a_{H_2O})\ (1 + C)\ (R - 1) \quad (14)$$

This is a simple first-order differential equation whose solution is

$$Y = \ln\,(1 - R) = Bt + A \quad (15)$$

Other rate equations were developed for other models shown in Table 1 both on the basis of activities and concentrations. Model *C* represents two second-order simultaneous competing reactions, while Model *E* represents a third-order reaction. Model *D* is a mechanism analogous to that proposed by Danckwerts and Melkerson (*15*) for the reaction of carbon dioxide with OH^-:

$$HS^*O_3^- \rightleftharpoons S^*O_2 \cdot OH^- \quad (16)$$

$$S^*O_2 \cdot OH^- + SO_2 \rightleftharpoons SO_2 \cdot OH^- + S^*O_2 \quad (17)$$

The detailed derivations can be found in reference *26*. Table 2 lists the integrated rate equations embodying the forward rate constants for the models in Table 1; a similar set of equations was developed which included the reverse rate constants.

EXPERIMENTAL

The equipment used in this study consisted of the following three major parts: the reaction vessel and sampling apparatus, shown in Figure 1; the Bernstein-Ballentine gas transfer apparatus (*3*); and standard radio counting equipment.

Prior to each run the radioactive material in the reaction vessel and the sampling system from the previous run had to be removed so as to avoid contamination of the apparatus. Sample bulbs, flash bulbs, liquid traps, and gas-collecting tubes were reassembled and given a preliminary check for vacuum retention. Previously prepared sodium bisulfite solution of proper normality was poured into the reaction vessel

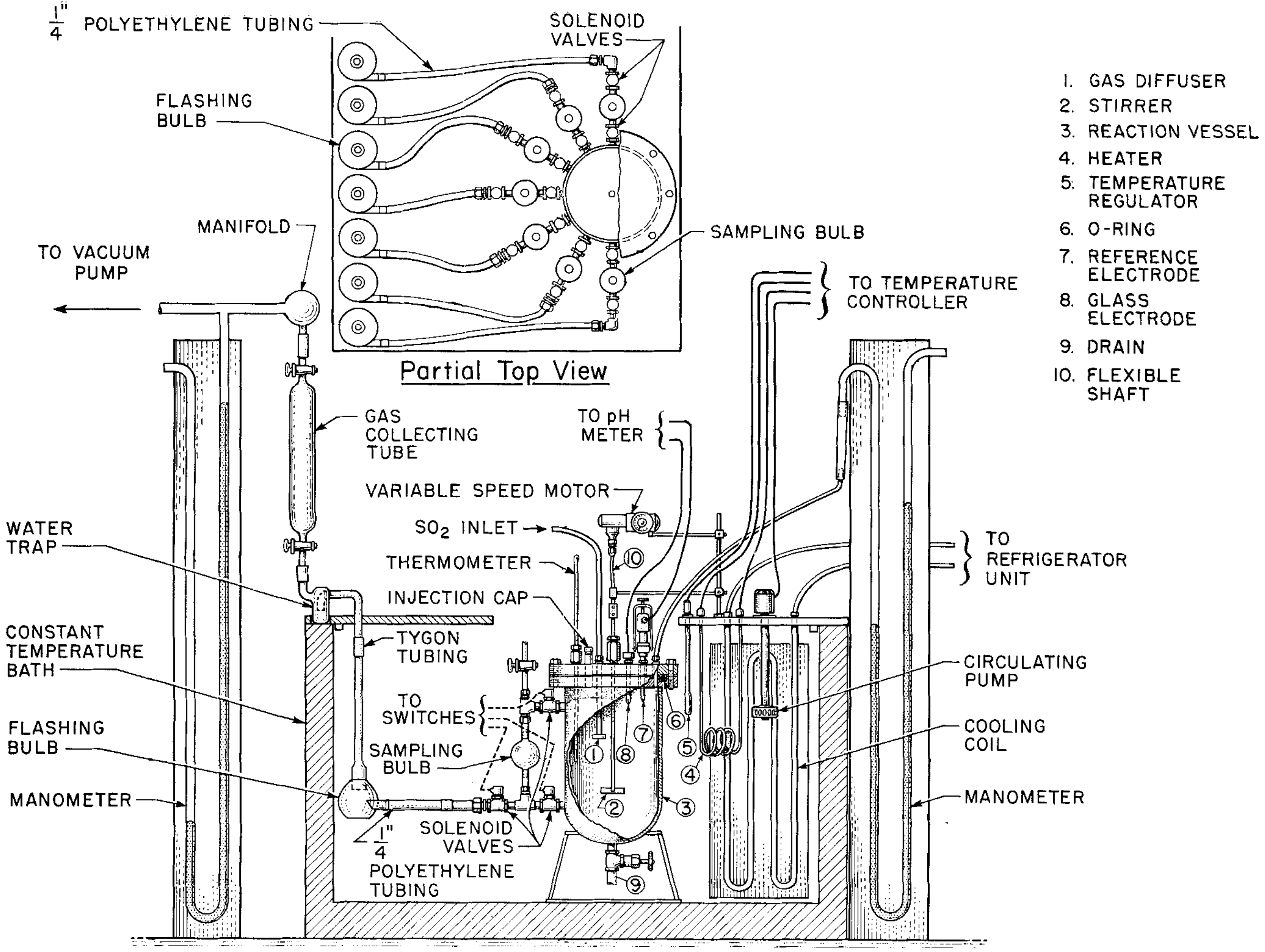

Fig. 1. Reaction vessel, sampling system and accessories.

until only about one-quarter of an inch of gas space remained over the liquid. Then the lid was bolted to the vessel, and the standardized pH electrodes, stirrer, manometer, etc. were engaged into their respective gland assemblies.

The system was purged with a sulfur dioxide-nitrogen mixture, and the pH, pressure, and temperature were periodically recorded to determine when equilibrium had been achieved.

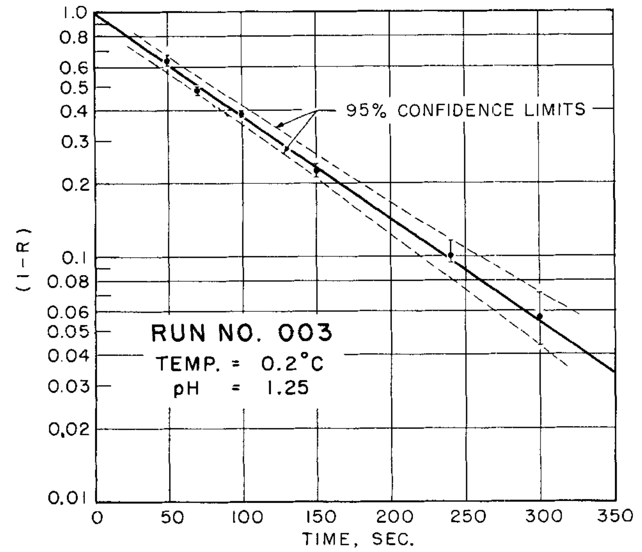

Fig. 2. Results from radioactive tracer counting data.

To start a run the stirrer was turned to full speed, and prepared tracer solution was injected by a hypodermic. After a mixing time of 20 to 30 sec. the liquid phase samples were drawn into the sample bulbs by a mercury displacement method which insured collection of liquid samples without flashing.

At periodic intervals the solenoid valve to the proper sample bulb was opened, and the liquid was allowed to run into the flash bulb from which the gas passed through a trap and then into a gas-collecting tube. Six gas samples were taken within 4 to 5 min., while a final sample was taken 2 to 3 hr. after the injection of tracer; this sample could be considered to be at isotopic equilibrium. The gas samples were later run through the Bernstein-Ballentine apparatus so they might be counted.

Two liquid samples were taken from the equilibrium solution to determine the amount of total sulfur dioxide (that is the

TABLE 1. SUMMARY OF REACTION MODELS

Reaction	Model
$SO_2 + H_2O \underset{k_R}{\overset{k_F}{\rightleftharpoons}} H^+ + HSO_3^-$	*A*
$SO_2 + OH^- \underset{k_r}{\overset{k_f}{\rightleftharpoons}} HSO_3^-$	*B*
A and *B* proceeding simultaneously.	*C*
$HS^*O_3^- \underset{k_{-a}}{\overset{k_a}{\rightleftharpoons}} S^*O_2 \cdot OH^-$ (Danckwert's model)	*D*
$2SO_2 + OH^- + H_2O \underset{k_{-2}}{\overset{k_2}{\rightleftharpoons}} H^+ + 2HSO_3^-$	*E*

Table 2. Summary of Integrated Rate Equations for Different Models

Model	Integrated rate equation	B*
A	$\ln(1-R) = B_A t + A_A$	$-[k_F(a_{H_2O})](1+C)$
B	$\ln(1-R) = B_B t + A_B$	$-[k_f(a_{OH^-})](1+C)$
C	$\ln(1-R) = B_C t + A_C$	$-[k_F(a_{H_2O}) + k_f(a_{OH^-})](1+C)$
D	$\ln(1-R) = B_D t + A_D$	$-\left[k_F \frac{\gamma_{(S^*O_2)e}}{\gamma_{1\ddagger}}(a_{H_2O}) + k_a \frac{\gamma_{HSO_3^-}}{\gamma_{2\ddagger}} \frac{1}{C}\right](1+C)$
E	$\ln \frac{(FR+E)}{(1-R)} = 2DEK_2t + A_G$	$D = [OH^-][H_2O]/[S^*O_2]_e$ $E = 1 + C$ $F = 1 - C$

* Expressions for B are given for rate equations derived on the basis of activities. Concentrations may be introduced as alternate variables if suitable activity coefficients are employed.

amount of sulfur dioxide plus HSO_3^-), as well as the concentration of sulfur dioxide and HSO_3^- so that the value of the constant C could be evaluated. The value of $R = (S^*O_2)/(S^*O_2)_e$ was obtained from the corrected radioactive counting data.

RESULTS AND CALCULATIONS

A statistical program for the CDC-1604 computer was used to find the parameters of the integrated rate equations in Table 2. Thirty experimental runs were carried out at five different temperatures: 0.2°, 5.0°, 10.0°, 15.0°, and 20.0°C. The concentrations of $NaHSO_3$ used in these runs ranged from 0.02 to 0.8 mole/liter, and the pH range was from 1.25 to 4.3, corresponding to a range of hydrogen ion concentration of 5.6×10^{-2} to 6×10^{-6} mole/liter. The hydrogen ion concentration was controlled by adjusting both the bisulfite concentration and the solution pressure. Figure 2 shows the type of data developed for a sample run and indicates the general overall accuracy experienced. Figure 3 shows the slope B as a function of pH. Data were limited to a pH range of 1.2 to 4.2 because the reaction rate at low pH was too fast to follow successfully, while a pH of greater than 4.2 reduced the concentration of sulfur dioxide in solution to below the convenient level for sampling. Details of the experimental data, results of calculations, and results of the statistical analysis may be found in reference *26*.

Figure 4 demonstrates that Model E did not represent the data very well, since each of the models called for a linear relationship between Y (the left-hand side of the integrated rate equations in Table 2) and t, a characteristic found to be true only for models A through D.

Next to get the individual rate constants it was necessary to use the data collected at different pH values and ionic concentrations. Values of $B/(1 + C)$ were analyzed statistically to see if they were constant (Model A), varied with a_{OH^-} or $[OH^-]$ (Models B and C), or varied with $1/C$ (Model D). Figure 5 is a graphical presentation for Model C (based on activities) of the results of one such regression analysis. Table 3 summarizes some of the results of these statistical analyses for Model C for both forward and reverse rate constants. In Table 3 correlation 1 (which devolves from the rate equations for Model C expressed in terms of activities) permitted the slope and intercept of the function $-[k_F(a_{H_2O}) + k_f(a_{OH^-})]$ plotted vs. a_{OH^-} to be evaluated, yielding the individual rate coefficients. Correlation 2 is the same except that the rate equations have been expressed in terms of concentrations

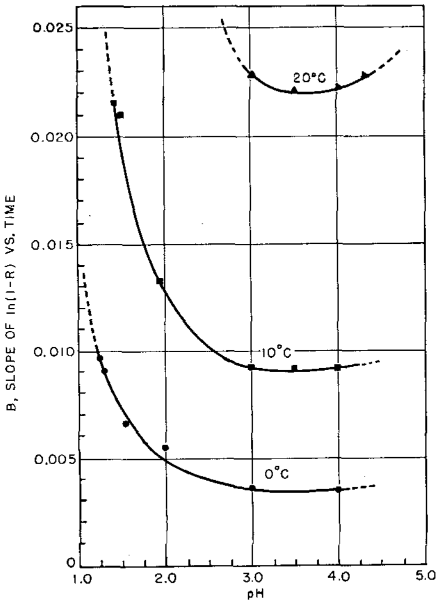

Fig. 3. Variation of rate of isotopic exchange with pH.

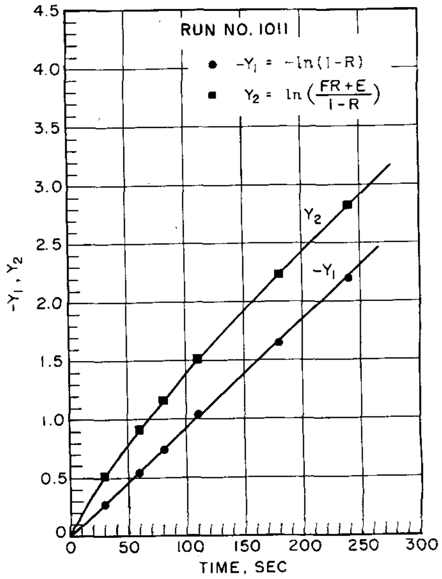

Fig. 4. Comparison of the integrated rate equations for different reaction models.

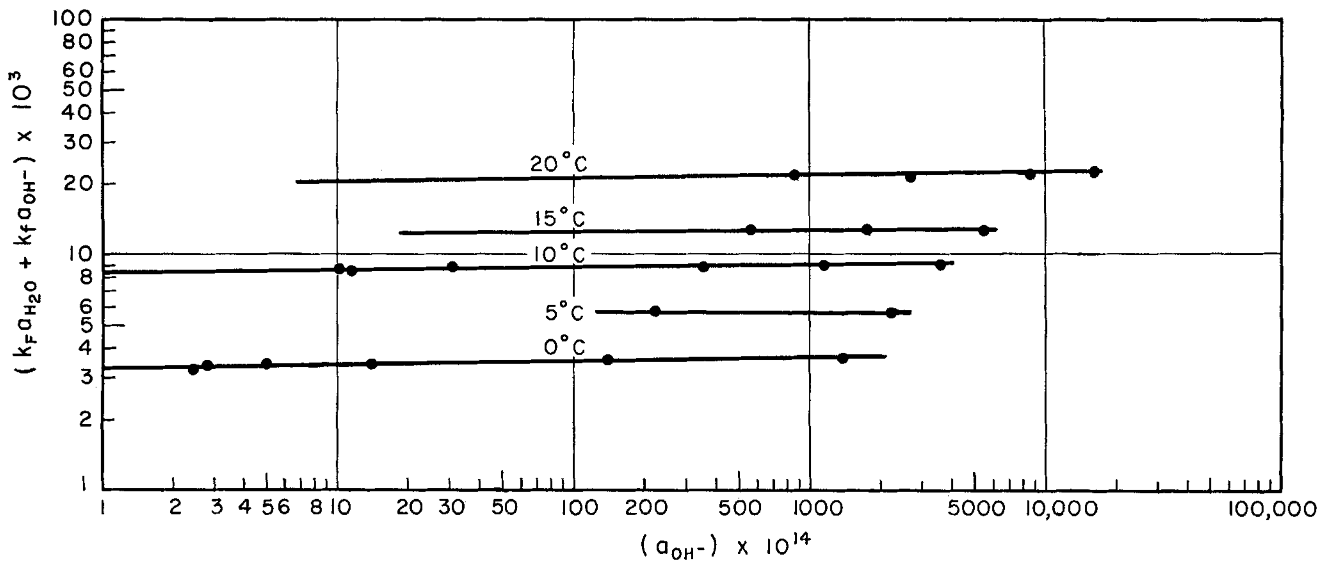

Fig. 5. Correlation of forward reaction rate data with hydroxyl ion activity.

instead of activities. Correlation 3 permitted evaluation of the reverse rate coefficients for Model *C* expressed in terms of concentrations.

DISCUSSION

Although in Figure 5 the lines appear to slope upward slightly as the a_{OH^-} increases, it was impossible to demonstrate statistically that k_f (or k_r) was significantly different from zero in this study. By analogy of sulfur dioxide to carbon dioxide and other like gases a reaction with OH^- is presumed to exist, but the contribution to the overall rate from this source was so small in this investigation that in effect it could not be detected. As a guess one might venture that the order of magnitude of k_f is similar to that for carbon dioxide in OH^- solutions.

For Model *C* no difference could be observed between models based on activity and those based on concentration because of a peculiarity in the estimated activity coefficients γ_{OH^-} and γ_{H^+}. In the pH range employed in this study these coefficients varied very slowly with concentration. Consequently changing the independent variable for correlation from a_{OH^-} to $[OH^-]$ for example merely shifted the horizontal scale leftward in Figure 5; since the slope of the line was so close to zero, the intercept, which essentially is k_F or k_{Fc}, remained unchanged.

One might think that certainly a difference could be detected between Models *C* and *D*, but as the following algebraic manipulation shows

$$K_a = \left(\frac{\gamma_{H^+}\,\gamma_{HSO_3^-}}{\gamma_{SO_2}}\right)\left(\frac{[H^+]\,[HSO_3^-]}{[SO_2]}\right) \quad (18)$$

$$K_w = \left(\frac{\gamma_{H^+}\,\gamma_{OH}}{a_{H_2O}}\right)[H^+]\,[OH^-] \quad (19)$$

$$\frac{1}{C} = \frac{[HSO_3^-]}{[SO_2]} = \frac{K_a}{K_w}\left[\frac{\dfrac{\gamma_{H^+}\,\gamma_{OH^-}}{a_{H_2O}}}{\dfrac{\gamma_{H^+}\,\gamma_{HSO_3^-}}{\gamma_{SO_2}}}\right][OH^-] \quad (20)$$

TABLE 3. RESULTS OF VARIOUS CORRELATIONS OF REACTION RATE CONSTANTS FOR MODEL *C*

Correlation	Temp., °C.		Slopes: Estimate	Slopes: 95% confidence Limits	Intercepts: Estimates	Intercepts: 95% confidence Limits	
1. $-B/(1+C)$ vs. a_{OH^-}	0.2	k_f	1.32×10^7	±159%	3.42×10^{-3}	±3.6%	k'_F
	5.0*				5.77×10^{-3}	±14.0%	
	10.0		0.96×10^7	±69%	8.79×10^{-3}	±1.5%	
	15.0		-0.42×10^7	±327%	12.99×10^{-3}	±4.1%	
	20.0		0.57×10^7	±116%	21.75×10^{-3}	±3.0%	
2. $-B/(1+C)$ vs. $[OH^-]$	0.2	k_{fc}	8.61×10^8	±118%	3.42×10^{-3}	±3.6%	k'_{Fc}
	5.0*				5.77×10^{-3}	±14.0%	
	10.0		6.39×10^8	±67%	8.79×10^{-3}	±1.5%	
	15.0		-2.69×10^8	±370%	12.99×10^{-3}	±1.9%	
	20.0		3.64×10^8	±118%	21.76×10^{-3}	±2.9%	
3. $-BC/(1+C)$ vs. $[H^+]$	0.2	k_{rc}	3.13×10^{-6}	±617%	0.144	±5.2%	k_{Rc}
	0.5*				0.209		
	10.0		64.22×10^{-6}	±317%	0.359	±3.1%	
	15.0		-0.12×10^{-6}	±1000%	0.592	±3.5%	
	20.0		0.77×10^{-6}	±1000%	1.121	±1.7%	

* Values at 5.0°C. are obtained from the average value of the two available runs:

$k'_F = k_F(_{H_2O})$; $k'_{Fc} = k_F[H_2O]$

TABLE 4. COMPARISON OF RATE CONSTANTS FOR REACTION WITH WATER

t, (°C.)	k'_F, (sec.$^{-1}$) $\times 10^3$ CO_2 (13)	SO_2	$k_R \frac{\text{liter}}{(\text{mole})(\text{sec.})}$ CO_2 (13)	SO_2
0	1.9	3.4	0.74×10^4	0.15
20	15	22	3.3×10^4	1.6

the quantity $1/C$ is directly proportional to the $[OH^-]$ inasmuch as it can be shown by experimental data (*12, 25*) that the ratio of the activity coefficient products under the conditions of this study was essentially a constant.

The temperature dependence of the rate constants for Model A as computed by the CDC-1604 computer was

$$\ln k_{F'} = 21.05 - 7{,}301\ (1/T) \quad (21)$$

$$\ln k_R = 32.79 - 9{,}469\ (1/T) \quad (22)$$

Over this short temperature range these equations fit the data quite well, but one might prefer to use an Othmer (*19*) correlation to extrapolate the data to higher temperatures.

As mentioned previously there were no kinetic data in the literature on the reaction of sulfur dioxide with water, and therefore no comparison can be made between the reaction rate constants determined in this study and those of other investigators. However there are some data for the equilibrium constant for reaction (*2*). Tartar and Garretson (*25*) and Johnstone and Leppla (*14*) reported thermodynamic equilibrium constants based on activities, while Davis (*7*) and Morgan and Maass (*18*) based their equilibrium constants on concentration units. Figure 6 compares the results of this work with the other four investigators for the two constants:

$$K_a = \frac{k'_F}{k_R} \quad (23)$$

$$K_c = \frac{k'_{Fc}}{k_{Rc}} \quad (24)$$

It is also of interest to compare the rate constants for reaction (2) (based on activities) with the constants for the corresponding reaction with carbon dioxide as in Table 4. Although the forward rate constants are of the same order of magnitude, the reverse rate constants are 10^4 times as large as those for carbon dioxide.

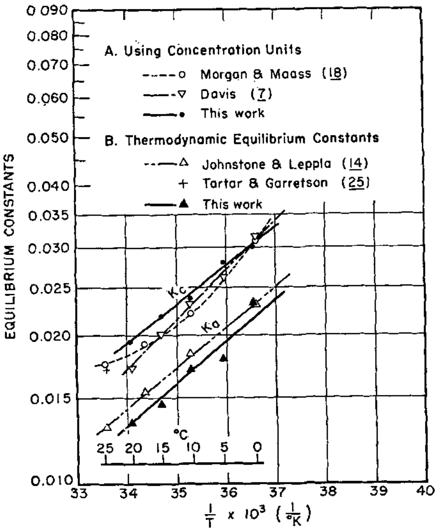

Fig. 6. Comparison of equilibrium constants with those of other investigators.

NOTATION

a = activity of species indicated by subscript
A = integration constant in various integrated rate equations
B = slope of the best straight line obtained by least-square fit of the experimental data points
C(alone) = ratio of sulfur dioxide concentration to HSO_3^- concentration at chemical equilibrium
C(with subscript) = concentration of components indicated by subscripts
D = diffusivity, sq. cm./sec.
k_2, k_{-2} = forward and reverse rate constant in concentration units of the reaction $2SO_2 + OH^- + H_2O \rightleftharpoons H^+ + 2HSO_3^-$, liter/(mole)^3 (sec.), and liter/(mole)^2 (sec.), respectively
k_a, k_{-a} = forward and reverse reaction rate constants of the Danckwerts model, (mole)/(liter) (sec.)
k_f, k_r = forward and reverse rate constant of the reaction $SO_2 + OH^- \rightleftharpoons HSO_3^-$ as expressed in activities, sec.$^{-1}$
k_{fc}, k_{rc} = forward and reverse rate constants in concentration units for the reaction $SO_2 + OH^- \rightleftharpoons HSO_3^-$ liter/(mole) (sec.), and sec.$^{-1}$, respectively
k_F, k_R = forward and reverse rate constants of the reaction $SO_2 + H_2O \rightleftharpoons H^+ + HSO_3^-$ as expressed in activities, sec.$^{-1}$
k_{Fc}, k_{Rc} = forward and reverse rate constants in concentration units of the reaction $SO_2 + H_2O \rightleftharpoons H^+ + HSO_3^-$, liter/(mole) (sec.)
K_a = thermodynamic equilibrium constant of the reaction $SO_2 + H_2O \rightleftharpoons H^+ + HSO_3^-$
K_c = equilibrium constant in concentration units for the reaction $SO_2 + H_2O \rightleftharpoons H^+ + HSO_3^-$
K_w = thermodynamic equilibrium constant of the reaction $H_2O \rightleftharpoons H^+ + OH^-$
R = ratio of S-35 in the counting gas at time t to that at isotopic equilibrium
t = time of reaction, sec.
t = temperature, °C.
T = temperature, °K.
Y = dependent variable in the correlations of the reaction rate constants
$\gamma_1^{\neq}$ = activity coefficient of an intermediate Brönsted complex
$\gamma_2^{\neq}$ = activity coefficient of the activated complex $(S^*O_2 \cdot OH^-)$

Subscripts

i = initial
e = at isotropic equilibrium
t = at time t

Superscripts

$*$ = radioactive species, that is S-35
$'$ = pseudo rate constants

Other

[ ] = concentration of reaction species indicated in the bracket

LITERATURE CITED

1. Anderson, L. B., and H. F. Johnstone, *A.I.Ch.E. Journal*, **1**, 135 (1959).
2. Astarita, G., and W. J. Beek, *Chem. Eng. Sci.*, **17**, 665 (1962).
3. Bernstein, W., and R. Ballentine, *Rev. Sci. Instr.*, **21**, 158 (1950).

4. Campbell, W. B., and O. Maass, *Can. J. Res.*, **2**, 42 (1930).
5. Chertkov, B. A., *Khim. Prom.*, **1959**, No. 7, p. 586 (1959).
6. Danckwerts, P. V., and K. A. Melkersson, *Trans. Faraday Soc.*, **58**, 1832 (1962).
7. Davis, D. S., *Chem. and Met. Eng.*, **39**, 615 (1932).
8. Falk, M., and P. A. Giguère, *Can. J. Chem.*, **36**, 1124 (1958).
9. Gerding, H., and W. J. Nijveld, *Rec. Trav. Chim.*, **56**, 968 (1937).
10. Getman, F. H., *J. Phys. Chem.*, **30**, 266 (1926).
11. Guyer, A., W. Richarz, and A. Guyer, Jr., *Helv. Chem. Acta.*, **38**, 1192 (1955).
12. Harned, H. S., and B. B. Owen, "The Physical Chemistry of Electrolytic Solutions," Reinhold, New York (1958).
13. Himmelblau, D. M., and A. L. Babb, *A.I.Ch.E. Journal*, **4**, 143 (1958).
14. Johnstone, H. F., and P. W. Leppla, *J. Am. Chem. Soc.*, **56**, 2233 (1934).
15. Kielland, J., *J. Am. Chem. Soc.*, **59**, 1675 (1937).
16. Lynn, S., J. R. Straatemeir, and H. Krammers, *Chem. Eng. Sci.*, **4**, 49 (1955).
17. Moelwyn-Hughes, E. A., "The Kinetics of Reactions in Solution," Oxford University Press, Oxford, England (1927).
18. Morgan, C. M., and O. Maass, *Can. J. Res.*, **5**, 162 (1931).
19. Othmer, D. F., *Ind. Eng. Chem.*, **32**, 841 (1940).
20. Rao, B. P., *Proc. Indian Accad. Sci.*, **A20**, 292 (1944).
21. Sherwood, T. K., and F. A. L. Hollaway, *Trans. Am. Inst. Chem. Engrs.*, **36**, 21 (1940).
22. Simon, A., and K. Waldmann, *Z. anorg. u. allgem. Chem.*, **281**, 113 (1955).
23. *Ibid.*, **283**, 359 (1956).
24. *Ibid.*, **284**, 36 (1956).
25. Tartar, H. V., and H. H. Garretson, Jr., *J. Am. Chem. Soc.*, **63**, 808 (1941).
26. Wang, J. C., Ph.D. thesis, Univ. Texas, Austin, Texas (1963).
27. Whitney, R. P., and J. E. Vivian, *Chem. Eng. Progr.*, **45**, 323 (1949).
28. ———, S. T. Han, and J. C. Davis, *Tappi*, **36**, 172 (1952).
29. Wright, R. J., *J. Chem. Soc.*, **105**, 2907 (1914).

Manuscript received June 17, 1963; revision received November 20, 1963; paper accepted November 21, 1963.

Heat Transfer Coefficients for a Hot Gas Oscillating at High Amplitudes in a Cylindrical Chamber

M. D. HORTON, J. L. EISEL, and G. L. DEHORITY

U.S. Naval Ordnance Test Station, China Lake, California

It has been noted that heat transfer from a fluid to a tube is much enhanced if the fluid is vibrating (*1*, *7*, *9*). This enhancement is of interest for several reasons, one of which is the use of oscillations to increase the efficiency of a heat exchanger. Also flame-generated oscillations can occur in ramjet engines, and the increased heat transfer may be detrimental to the durability of the combustion chamber.

Furthermore a phenomenon known as *oscillatory combustion* is encountered in the course of many rocket development programs. This phenomenon occurs when the combustion process supports oscillations of the combustion gas in the rocket motor. Usually the oscillations are in acoustic modes of the combustion chamber and may be sensed by high-frequency response pressure-recording instrumentation. Frequently these oscillations are driven to very high amplitudes, and they are harmful to both the performance of the motor and its structural integrity. Part of the harm results from increased heat transfer, part from the change in mean pressure caused by interaction of the oscillations and combustion process, and part from the hammering action of the oscillations.

While there have been measurements made of the heat transfer coefficient which exists in a combustion tube in the presence of low-amplitude oscillations (*9*), such measurements taken in the presence of high amplitude oscillations are lacking. This is because high-amplitude oscillations are generally encountered in the combustion system of rocket motors, and in the presence of the high temperature, chemically-reactive environment which exists in the rocket combustion chamber measurements of all kinds are difficult to make. Measurements of the heat transfer coefficient would be desirable because they would aid in hardware design, and they would also augment the present heat transfer literature.

This paper presents some estimates of the average heat transfer coefficient which exists in the presence of a high-temperature gas oscillating at high amplitudes in a cylindrical steel cavity. The measurements were taken over the frequency range of 600 to 8,000 cycles/sec. and in the presence of decaying oscillations which ranged approximately from a peak to peak amplitude of 30 down to 2 lb./sq.in.

EXPERIMENT

Inasmuch as the treatment of the data is so dependent upon the special conditions which exist in this experiment, the experiment will be described before the data reduction is described.